

Adaptive Neuro Fuzzy Inference Controller for Full Vehicle Nonlinear Active Suspension Systems

A. Aldair and W. J. Wang

*School of Engineering and Design, University of Sussex,
Falmer, East Sussex, BN1 9QT, UK*

aa386@sussex.ac.uk

w.j.wang@sussex.ac.uk

Abstract— The main objective of designed the controller for a vehicle suspension system is to reduce the discomfort sensed by passengers which arises from road roughness and to increase the ride handling associated with the pitching and rolling movements. This necessitates a very fast and accurate controller to meet as much control objectives, as possible. Therefore, this paper deals with an artificial intelligence Neuro-Fuzzy (NF) technique to design a robust controller to meet the control objectives. The advantage of this controller is that it can handle the nonlinearities faster than other conventional controllers. The approach of the proposed controller is to minimize the vibrations on each corner of vehicle by supplying control forces to suspension system when travelling on rough road. The other purpose for using the NF controller for vehicle model is to reduce the body inclinations that are made during intensive manoeuvres including braking and cornering. A full vehicle nonlinear active suspension system is introduced and tested. The robustness of the proposed controller is being assessed by comparing with an optimal Fractional Order $PI^{\lambda}D^{\mu}$ (FOPID) controller. The results show that the intelligent NF controller has improved the dynamic response measured by decreasing the cost function.

Keywords: Full vehicle, nonlinear active suspension system, neuro-fuzzy system, control design.

I. INTRODUCTION

A number of researchers have suggested control methods for vehicle suspension systems. Some have designed a linear controller for a quarter or half vehicle [1-9]. In reference [10] the authors used a robust controller for a full vehicle linear active suspension system using the mixed parameter synthesis. A sliding mode technique is designed for a linear full vehicle active suspension system [11]. A method is

developed for the purpose of sensor fault diagnosis and accommodation. In reference [12] the authors presented the development of an integrated control system of active front steering and normal force control using fuzzy reasoning to enhance the full vehicle model handling performance. A fuzzy logic based fast gain scheduling controller is proposed for control nonlinear suspension systems for quarter car system [13]. In fact, nonlinearity inherently exists in damper and spring models [14-16]. Therefore, the nonlinear effect should be inevitably taken into account to design the controller for practical active suspension system.

This paper will be developed a novel NF controller for full vehicle nonlinear active suspension systems. The full vehicle model will be investigated to take into account the three motions of the vehicle: vertical movement at centre of gravity, pitching movement and rolling movement. It is believed that, this is the first time to use the neuro-fuzzy method to design the controller for a full vehicle nonlinear active suspension system.

A neurofuzzy model combines the features of a neural network and fuzzy logic model. A large class of neuro-fuzzy approaches utilizes the neural network learning algorithms to determine parameters of the fuzzy logic system [17]. The neuro-fuzzy system is more efficient and more powerful than either neural network or fuzzy logic system [18] which has been widely used in control systems, pattern recognition, medicine, expert system, etc. [19].

In this paper optimal FOPID controller will be designed for full vehicle nonlinear active suspension by using the Evolutionary Algorithm (EA). The data obtained from the optimal FOPID controller will be used as reference to design the NF controller. The learning ability of the neural network has been used to tune parameters of the membership function of the Fuzzy Inference Systems (FIS). The performance of the NF controller has been improved by adding the scaling gains. The results of the proposed controller will be compared with

that of the optimal FOPID controller. Four types of the disturbances will be investigated to establish the robustness of the proposed controller:

- Change the amplitude of the sine shape of the road profile input.

Change the amplitude of the square shape of the road profile input.

- Change the bending inertia torque with random road profile input.
- Change the breaking inertia torque with random road profile input.

The results will show whether the proposed controller is more robust than the optimal FOPID controller.

II. THE STRUCTURE AND TRAINING OF ADAPTIVE NEURO FUZZY INFERENCE SYSTEM (ANFIS)

The ANFIS is one of the methods to organize the fuzzy inference system with given input/output data pairs. The ANFIS is a combination of a fuzzy logic controller and a neural network, which makes the controller self tuning and adaptive. If we compose these two intelligent approaches, it will be achieve good reasoning in quality and quantity. This technique gives the fuzzy logic capability to adapt the membership function parameters that best allow the associated fuzzy inference system to track the given input/output data. The data obtain from FOPID controller will be use to modify the parameters of ANFIS model. In order to process a fuzzy rule by neural networks, it is necessary to modify the standard neural network structure accordingly. Fig. 3 depicts the structure of Neuro-fuzzy inference system (the type of this model is called Takagi-Sugeno-Kang) [20]. For the simplicity, the following assumptions will be assumed: (a) the model has two inputs x and y and one output z , (b) it has just two rules ($R1$ and $R2$).

$R1$: If x is A_1 and y is B_1 then $f_1 = p_1x + q_1y + r_1$

$R2$: If x is A_2 and y is B_2 then $f_2 = p_2x + q_2y + r_2$

In Fig. 1, square nodes (adaptive nodes) have adaptable parameters while circle nodes (fixe nodes) have non-adaptable parameters. The function of each layer is described below:

Layer 1: Every node i in this layer is a square node with a node function

$$O_i^1 = \mu_{C_i}(w) \quad i=1, 2 \quad (1)$$

where w is the input to the node i (x or y) and C_i is the linguistic label associated with this node (A_i or B_i).

$\mu_{C_i}(w)$ has been chosen as Bell-Shape membership function:

$$\mu_{C_i}(w) = \frac{1}{1 + \left[\frac{w - c_i}{a_i} \right]^{2b_i}}$$

where $\{a_i, b_i, c_i\}$ are the parameters of membership function (they are called premise parameters) which will be modified in the training phase.

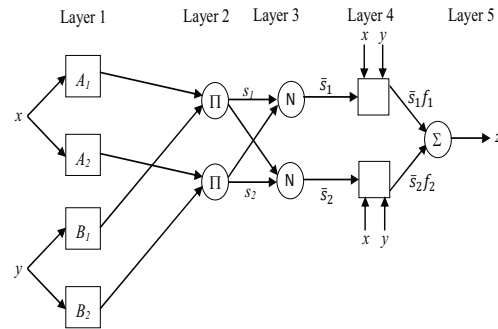


Fig. 1 ANFIS model

Layer 2: Every node in this layer is a circle node (have non-adaptable parameters) labeled Π which multiplies the incoming signals. The output of each node in this layer can be written as:

$$O_i^2 = s_i = \mu_{A_i}(x) \times \mu_{B_i}(y) \quad i=1, 2 \quad (2)$$

Layer 3: Every node in this layer is a circle node labeled N . the output of i^{th} node is the normalized of the i^{th} rule's firing strength. The output of any node in this layer can be given as

$$O_i^3 = \bar{s}_i = \frac{s_i}{s_1 + s_2} \quad (3)$$

Layer 4: Every node in this layer is square node with linear function

$$f_i = p_i x + q_i y + r_i \quad (4)$$

where $\{p_i, q_i, r_i\}$ is the set parameters of linear equation (they are called consequent parameters) which will be modified in the training phase. The output of any node in this layer can be written as:

$$O_i^4 = \bar{s}_i f_i = \bar{s}_i (p_i x + q_i y + r_i) \quad (5)$$

Layer 5: the node in this layer is circle nod labeled Σ that compute the overall output as the summation of all incoming signals

$$z = O_i^5 = \sum_i \bar{s}_i f_i = \frac{\sum_i s_i f_i}{\sum_i s_i} \quad (6)$$

The adaptable parameters of ANFIS $\{a_i, b_i, c_i, p_i, q_i, r_i\}$ should be modified to minimize the following performance function:

$$E = \sum_{p=1}^P E_p \quad (7)$$

where P is the total number of training data set and E_p the error signal between the desired output of p^{th} data and the actual output of ANFIS model of p^{th} data, E_p can be given as

$$E_p = T_p - z_p \quad (8)$$

where T_p the p^{th} desired output and z_p the p^{th} actual output of the ANFIS model.

To modify the parameters of the ANFIS model, the steepest descent method as in neural network can be applied to modify the premise parameters $\{a_i, b_i, c_i\}$ and least square estimate can be applied to adapt the consequent parameters $\{p_i, q_i, r_i\}$ [21].

III. DESIGN OF THE NEURO-FUZZY CONTROLLER

The neuro-fuzzy controller is a combination of a fuzzy logic controller and a neural network, which makes the controller self tuning and adaptive. Fig. 2 depicts the Neuro-fuzzy controller with controlled system. The structure of the NF controller in this figure is described in previous section. To find the optimal values of the NF parameters (premise and consequent parameters) for driving the plant to meet all control objectives, a FOPID controller should be designed. The input/output data which will be obtained from FOPID controller design should be used to train the NF controller.

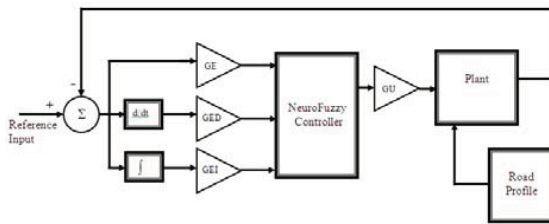


Figure 2. Neuro-Fuzzy Controller

A. FOPID Controller Design

In this paper Evolutionary Algorithm (EA) has been used to tune the parameters of FOPID controller. The continuous transfer function of FOPID controller is described as [22]

$$G_c(s) = \frac{U(s)}{E(s)} = K_p + \frac{K_i}{s^\lambda} + K_d s^\mu \quad (9)$$

Fig.3 depicts the structure of the multi-population evolutionary algorithm. At the beginning of the computation, a number of individuals (FOPID parameters) are randomly initialized within a reliable range. The first/initial generation is produced. If the optimization criteria are not met, the creation of a new generation starts. Individuals are selected according to their fitness for the production of offspring. The parents are recombined to produce offspring. All offsprings will be mutated with a certain probability. The fitness of the offspring is then computed. The offsprings are inserted into the population replacing the parents, producing a new generation. This cycle is performed until the optimization criteria are met. The objectives of modify the parameters of FOPID are to resolve the inherent conflict between riding comfort and road handling. Therefore, the FOPID parameters should be selected to minimize the following cost function,

$$J = 0.5 \sum_{\delta=1}^4 \xi_{\delta}^2 \quad (10)$$

where ξ_{δ} is the plant outputs which should be minimized.

B. Modifying the Parameters of NF Controller

After the optimal parameters of the FOPID controller are been obtained, the input/output data of the FOPID controller should be used to train the parameters of NF controller using the Hybrid Learning algorithm. Fig. 4 depicts the training phase of the NF controller.

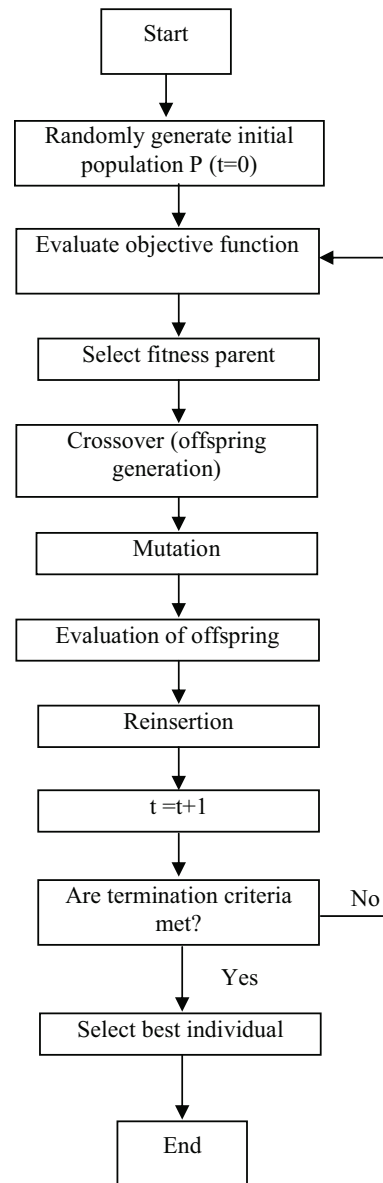


Figure 3. Structure of an evolutionary algorithm

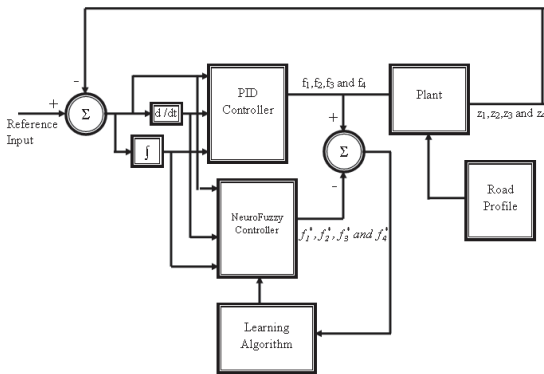


Fig. 4 Training Phase of NF Controller

The bold line means multiple input or output signals. After the optimal values of NF are obtained the NF controller design should be improved by adjusting the scaling gains (GE, GED, GEI and GU) as shown in Fig. 2.

IV. MATHEMATICAL MODEL OF THE CONTROLLED SYSTEM

A framework is suggested that the NF controller generates the suitable command signals (inputs of the hydraulic actuators) to improve the vehicle performance including riding comfort and road handling stability. The rigid comfort can be measured by evaluating the acceleration and displacement of the sprung mass. The handling stability can be obtained by minimizing the vertical motion of tires and the rotational motions of the vehicle body such as rolling and pitching movements during sharp manoeuvres cornering and braking.

The full vehicle active suspension physical model is shown in Fig. 5. This model consists of five parts: the sprung mass (M) and four unsprung masses m_i (where $i \in [1,2,3,4]$). The sprung mass is assumed as rigid body and has freedom of motion in vertical, pitch and roll direction. The vertical displacements at each suspension point are denoted by z_1, z_2, z_3 and z_4 . The z_c, α and η denote the displacement at the center of gravity of the vehicle, pitch angle and roll angle, respectively. The vertical displacements of unsprung masses are denoted by w_1, w_2, w_3 and w_4 . J_x and J_y are moments of inertia about x-axis and y-axis, respectively. The cornering torque and braking torque are denoted by T_x and T_y , respectively. In the model, the disturbances u_1, u_2, u_3 and u_4 are caused by road roughness.

A. Nonlinear Force Characteristics

The suspension elements possess a nonlinear property. Therefore, each suspension will be assumed as specify nonlinear components placed in parallel (nonlinear spring model, nonlinear damper model and nonlinear hydraulic actuator). The main purpose of using the suspensions control

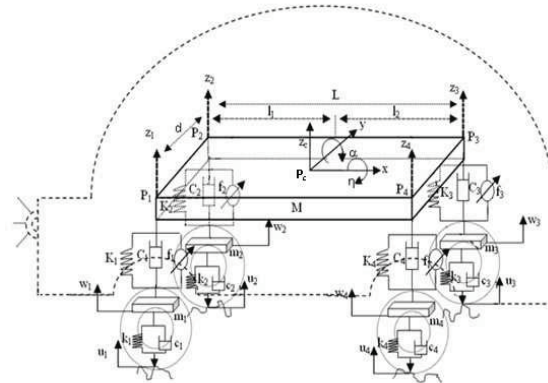


Figure 5. Full vehicle nonlinear active suspension system

is to generate a control force between sprung mass and unsprung masses. The i^{th} nonlinear suspension has stiffness and damping coefficient denoted by K_i and C_i , respectively. Each tire will be simulated as linear oscillator with stiffness and damping coefficient denoted by k_i and c_i , respectively. The motions of the sprung mass are governed by the following equations:

• Vertical motion

$$M\ddot{z}_c = -\sum_{i=1}^4 F_{Ki} - \sum_{i=1}^4 F_{Ci} + \sum_{i=1}^4 F_{Pi} \quad (11)$$

where F_{Ki} , F_{Ci} are nonlinear suspension spring forces and nonlinear suspension damping force, respectively, which can be written as [23]

$$F_{Ki} = K_i(z_i - w_i) + \xi K_i(z_i - w_i)^3$$

$$F_{Ci} = C_i(\dot{z}_i - \dot{w}_i) + \xi C_i(\dot{z}_i - \dot{w}_i)^2 \text{sgn}(\dot{z}_i - \dot{w}_i)$$

$F_{Pi} = F_{Ai} - F_{fi}$ where F_{Ai} nonlinear hydraulic force provided by the i^{th} actuator and F_{fi} the nonlinear frictional force due to rubbing of piston seals with the cylinders wall inside the i^{th} actuator.

• Pitching motion

$$J_x \ddot{\alpha} = (F_{K1} - F_{K2} - F_{K3} + F_{K4}) \frac{b}{2} + (F_{C1} - F_{C2} - F_{C3} + F_{C4}) \frac{b}{2} + (F_{P4} - F_{P1} + F_{P3} - F_{P2}) \frac{b}{2} + T_x \quad (12)$$

where b is the distance between the front wheels (or rear wheels).

• Rolling motion

$$J_y \ddot{\eta} = (F_{K3} + F_{K4})l_2 - (F_{K1} + F_{K2})l_1 + (F_{C3} + F_{C4})l_2 - (F_{C1} + F_{C2})l_1 + (F_{P1} + F_{P2})l_1 + (F_{P3} + F_{P4})l_2 + T_y \quad (13)$$

where l_1 is the distance between the centre of front wheel axle and centre of gravity of the vehicle. l_2 is the distance between the centre of gravity of the vehicle and the centre of rear wheel axle.

The motion of the i^{th} unsprung mass is governed by the following equation:

$$m_i \ddot{w}_i = -k_i(w_i - u_i) - c_i(\dot{w}_i - \dot{u}_i) + F_{Ki} + F_{Ci} - F_{Pi} \quad (14)$$

B. Hydraulic Actuator Dynamics

The nonlinear force produced by the active hydraulic actuator is applied between body and wheel axles. This force is governed by the following equation [24]

$$F_{Ai} = A_p P_{Li} \quad (15)$$

where A_p the cross section area of the piston inside the i^{th} actuator, P_{Li} the hydraulic pressure inside the i^{th} actuator. The nonlinear pressure is given by:

$$\dot{P}_{Li} = -\beta P_{Li} - \sigma(A_p \dot{x}_{pi} - Q_i) \quad (16)$$

where $\sigma = \frac{4\beta_e}{V_t}$, $\beta = \sigma C_{tp}$ and $x_{pi} = z_i - w_i$

β_e the effective bulk modulus of hydraulic system.

V_t the total volume of fluid under compression.

C_{tp} leakage coefficient of piston.

Q_i hydraulic flow through the piston inside the i^{th} actuator.

Q_i is governed by the following equation:

$$Q_i = C_d \omega x_{vi} \sqrt{\frac{1}{\rho}(P_{si} - \text{sgn}(x_{vi})P_{Li})} \quad (17)$$

where

C_d is the discharge coefficient,

ω is the area gradient,

x_{vi} is the spool valve displacement,

ρ is the fluid density,

P_s is the supply piston pressure.

The spool valve displacement is controlled by an input voltage u_m . The corresponding dynamic relation can be simplified as a first order differential equation:

$$\dot{x}_{vi} = \frac{1}{\tau}(u_{mi} - x_{vi}) \quad (18)$$

C. Friction Force

Due to rubbing of the piston with the inside actuator wall, heat energy is generated. Therefore, the actual force generated by the i^{th} hydraulic actuator F_{Ai} is not equal to the force supply by i^{th} hydraulic actuator F_{Pi} . Difference between

these two forces is called friction force F_{fi} . This frictional force can not be neglected because the value of this force is greater than 200 Nm [25].

Frictional force is modelled with a smooth approximation of Signum function

$$F_{fi} = \begin{cases} \kappa \text{sgn}(\dot{z}_i - \dot{w}_i) & \text{if } |\dot{z}_i - \dot{w}_i| > 0.01 \\ \kappa \sin\left(\frac{\dot{z}_i - \dot{w}_i}{0.01} \frac{\pi}{2}\right) & \text{if } |\dot{z}_i - \dot{w}_i| < 0.01 \end{cases} \quad (19)$$

D. Full State Space Model of Vehicle with Nonlinear Suspension

The suspensions points P_1 , P_2 and P_4 satisfy the plane equation

$$\begin{vmatrix} x - x_1 & y - y_1 & z - z_1 \\ x_2 - x_1 & y_2 - y_1 & z_2 - z_1 \\ x_4 - x_1 & y_4 - y_1 & z_4 - z_1 \end{vmatrix} = 0$$

Any points on the rigid plate satisfy

$$z = \frac{(z_4 - z_1)}{L}x + \frac{(z_2 - z_1)}{b}y + z_1 \quad (20)$$

The vertical displacement at centre of gravity z_c can be calculated from eq. (20) as following:

$$z_c = az_1 + 0.5z_2 + \frac{1}{L}z_4$$

where $a = 0.5 - \frac{l_2}{L}$ and $L = l_1 + l_2$

Applying eq. (20) at point P_3 , the displacement can be written as

$$z_3 = -z_1 + z_2 + z_4.$$

The pitch angle and the roll angle can be calculated from the following equations:

$$\alpha = \frac{\partial z}{\partial y} = \frac{z_2 - z_1}{b}$$

$$\eta = \frac{\partial z}{\partial x} = \frac{z_4 - z_1}{L}$$

For simplify, the following assumptions will be assume

$$s_i = (z_i - w_i)^3 \quad i \in \{1,2,3,4\}$$

$$s_j = (\dot{z}_i - \dot{w}_i)^2 \text{sgn}(\dot{z}_i - \dot{w}_i) \quad j \in \{5,6,7,8\}$$

$$s_r = x_{vi} \sqrt{\frac{1}{\rho}(P_{si} - \text{sgn}(x_{vi})P_{Li})} \quad r \in \{9,10,11,12\}$$

$$s_h = \begin{cases} \text{sgn}(\dot{z}_i - \dot{w}_i) & \text{if } |\dot{z}_i - \dot{w}_i| > 0.01 \\ \sin\left(\frac{\dot{z}_i - \dot{w}_i}{0.01} \frac{\pi}{2}\right) & \text{if } |\dot{z}_i - \dot{w}_i| < 0.01 \end{cases} \quad h \in \{13,14,15,16\}$$

The input in the state space is governed by the following equation:

$$\dot{X} = B_1 X + B_2 S + B_3 U \quad (21)$$

where B_1, B_2, B_3, C_0 and D are coefficients matrices of the suspension systems model.

The output equation can be written as:

$$Y = C_0 X + DU \quad (22)$$

TABLE 1. VEHICLE SUSPENSION PARAMETERS

$$\text{where } X = \begin{bmatrix} X_1 \\ X_2 \end{bmatrix}; U = \begin{bmatrix} U_1 \\ U_2 \end{bmatrix}$$

$$X_1 = \begin{bmatrix} z_c \\ \alpha \\ \eta \\ w_1 \\ w_2 \\ w_3 \\ w_4 \\ P_{L1} \\ P_{L2} \\ P_{L3} \\ P_{L4} \\ x_{v1} \\ x_{v2} \\ x_{v3} \\ x_{v4} \end{bmatrix}; X_2 = \begin{bmatrix} \dot{z}_c \\ \dot{\alpha} \\ \dot{\eta} \\ \dot{w}_1 \\ \dot{w}_2 \\ \dot{w}_3 \\ \dot{w}_4 \end{bmatrix}; S = \begin{bmatrix} s_1 \\ s_2 \\ s_3 \\ s_4 \\ s_5 \\ s_6 \\ s_7 \\ s_8 \\ s_9 \\ s_{10} \\ s_{11} \\ s_{12} \\ s_{13} \\ s_{14} \\ s_{15} \\ s_{16} \end{bmatrix}; U_1 = \begin{bmatrix} T_x \\ T_y \\ u_1 \\ u_2 \\ u_3 \\ u_4 \\ u_{m1} \\ u_{m2} \\ u_{m3} \\ u_{m4} \end{bmatrix}; U_2 = \begin{bmatrix} \dot{u}_1 \\ \dot{u}_2 \\ \dot{u}_4 \end{bmatrix}$$

Notation	Description	Values	Units
K_1, K_2	Front-left and Front-right suspension stiffness, respectively.	19960	N/m
K_3, K_4	Rear-right and rear-left suspension stiffness, respectively.	17500	N/m
k_1-k_4	Front-left, Front-right, rear-right and rear-left tire stiffness respectively.	175500	N/m
C_1, C_2	Front-left and Front-right suspension damping, respectively.	1290	N.sec/m
C_3, C_4	Rear-right and rear-left suspension stiffness, respectively.	1620	N.sec/m
c_1-c_4	Front-left, Front-right, rear-right and rear-left tire damping, respectively.	14.6	N.sec/m
M	Sprung mass.	1460	kg
m_1, m_2	Front-left, Front-right tire mass, respectively.	40	kg
m_3, m_4	Rear-right and rear-left tire mass, respectively.	35.5	kg
J_x	Moment of inertia x-direction.	460	kg.m ²
J_y	Moment of inertia y-direction.	2460	kg.m ²
l_1	Distance between the center of gravity of vehicle body and front axle.	1.011	m
l_2	Distance between the center of gravity of vehicle body and rear axle.	1.803	m
b	Width of vehicle body	1.51	m
	Empirical parameter	0.1	-
α, β, γ	Actuator parameters	4.515×10^{13} , 1, 1.545×10^9	-
A_p	Cross section area of piston	3.35×10^{-4}	m ²
	Supply pressure	10342500	Pa
	Time constant	1/30	sec
C_d	Discharge coefficient	0.7	-
ρ	Fluid density	970	kg/m ³
ω	Area gradient	1.436e-2	m ²

The output matrix can be given by

$$Y = [z_1 \ z_2 \ z_3 \ z_4 \ w_1 \ w_2 \ w_3 \ w_4 \ z_c \ \alpha \ \eta]^T$$

V. SIMULATIONS AND RESULTS

For the full vehicle nonlinear active suspension system discussed in Section 4, the numerical values of the hydraulic actuators and full the vehicle model which are used in this simulation are given in Table 1. To design the NF controller, the optimal parameters of FOPID controller should be obtained first using the EA. The input/output data obtained from the FOPID controller have been used to design the NF controller. Figures 6-10 show the changing of the FOPID controller parameters (proportional constant K_p , derivative constant K_d , integral constant K_i , integral order λ and derivative order μ) with respect to optimization steps. Fig. 11 shows the response of the cost function (which is described in Eq. 10) with respect to the optimization steps. After 225 optimization iteration steps, the optimal values of the FOPID controller parameters can be obtain as shown in Table 2.

TABLE 2. THE INITIAL AND OPTIMAL VALUES OF FOPID CONTROLLER PARAMETERS

Parameter	Initial value	Optimal value
K_p	100	12678.26
K_d	20	3253.92
K_i	1	768.1
λ	0.3	0.45
μ	0.7	0.886

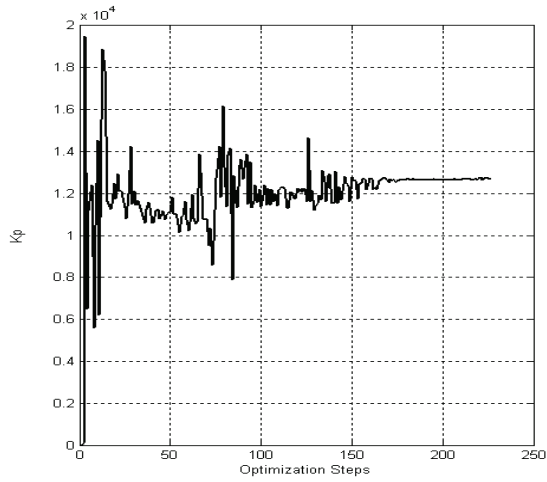


Figure 6. Changing value of K_p during optimization steps

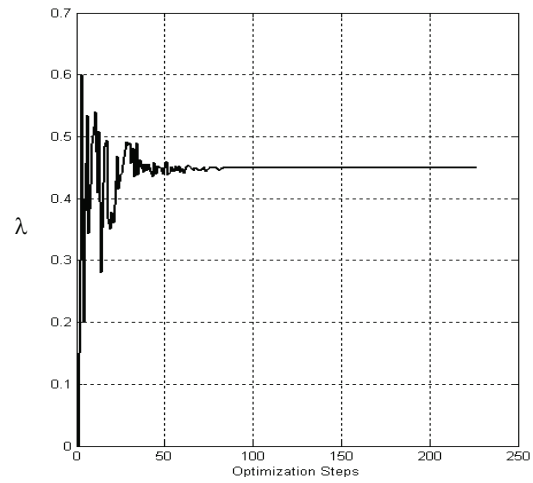


Figure 9. Changing value of λ during optimization steps

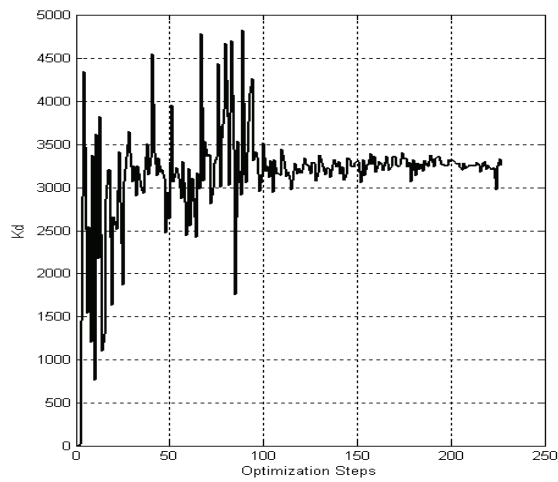


Figure 7. Changing value of K_d during optimization steps

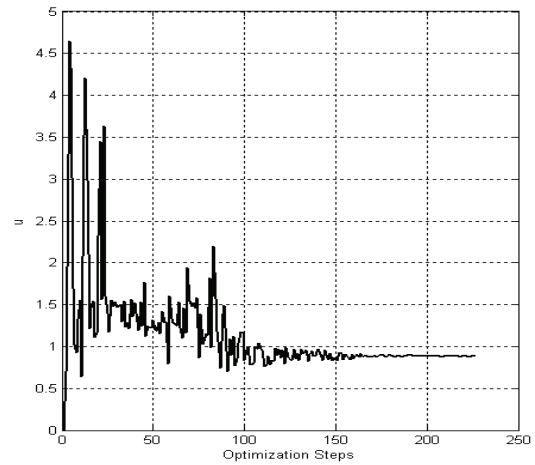


Figure 10. Changing value of μ optimization steps

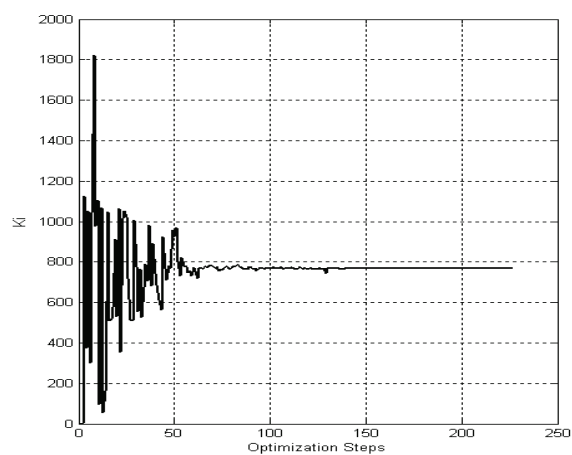


Figure 8. Changing value of K_i during optimization steps

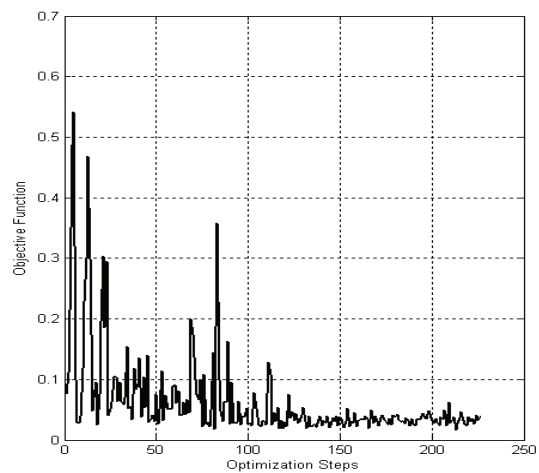


Figure 11. Performance measurement during optimization steps

After the optimal parameters of FOPID controller have been obtained, the input/output data should be used to design the NF controller. Fig. 4 shows the training phase of the NF controller. The NF controller consists of four NF sub-controllers (one controller for each suspension). The number of inputs for each NF sub-controller are three. The first input (Input 1) is the error between the vertical displacement at the corner where the NF sub-controller exists and desire vertical displacement. The second and the third input (Input 2 and Input 3) are derivative and integration of this error, respectively. The Bell-Shape function has been used for each NF sub-controller inputs. Input 1 has five grades: negative big (NB), negative small (NS), zero (ZE), positive small (PS) and positive big (PB). Input 2 has five grades: negative big (NB), negative small (NS), zero (ZE), positive small (PS) and positive big (PB). Input 3 has three grades: negative (N), no change (NCH) and positive (P). The Sugeno-Type fuzzy inference system has been used. The linear function has been used as output membership function. The output of each controller is the force controller. It has five grades: negative big (NB), negative small (NS), zero (ZE), positive small (PS) and positive big (PB). The following rules have been used

- R1: IF error is NB and errordot is NB and errorint N then force is NB**
- R2: IF error is NS and errordot is NS and errorint P then force is NS**
- R3: IF error is ZE and errordot is ZE and errorint NCH then force is ZE**
- R4: IF error is PS and errordot is PS and errorint P then force is PS**
- R5: IF error is PB and errordot is PB and errorint N then force is PB**

The selection of these rule depends on the response of the optimal FOPID controller. The Hybrid Learning algorithm has been used to select the optimal values for each NF controller.

To improve the performance of the NF controller the scaling gains should be adjusted. Fig.2 shows the NF controller with GE, GED, GEI and GU gains. The optimal values of scaling gains are 26, 22, 10 and 1.5, respectively.

Section 2 show that the vertical displacement at centre of gravity (z_c), the vertical displacement at P_3 (z_3), the pitching movement α and rolling movement η are depended on the vertical displacement at P_1 , P_2 and P_4 (z_1 , z_2 and z_4). Therefore, just the response at these points will be shown in this paper. In Figures (12-14) the time responses of the full vehicle nonlinear adaptive model without controller, optimal PID controller and NF controller at P_1 , P_2 and P_4 are compared, respectively. From these figures it can be shown that the NF controller is more powerful and efficient than the optimal PID controller.

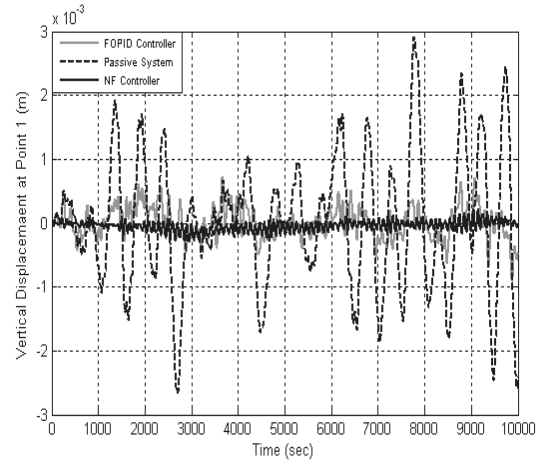


Figure 12 Time response of vertical displacement at P_1

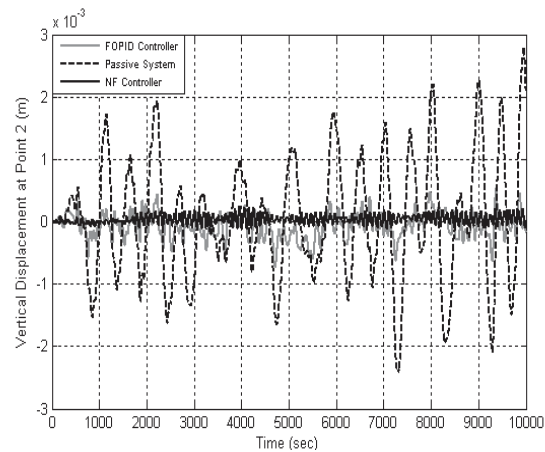


Figure 13 Time response of vertical displacement at P_2

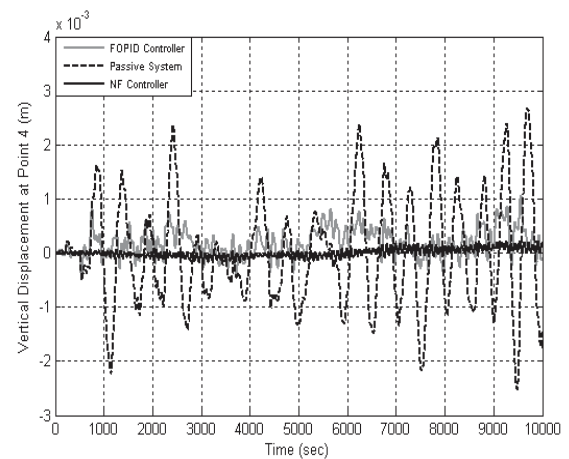


Figure 14 Time response of vertical displacement at P_4

VI. TEST OF ROBUSTNESS OF THE PROPOSED CONTROLLER

The efficient controller is the controller that it is still stable even the disturbance signal is applied on the plant. Therefore, to establish the effectiveness of any controller the robustness should be examined. Four types of disturbances are applied in turn to test the robustness of the NF controller.

A. Square input signal with varying amplitude applied as road input profile

The square input signal has been applied as road input. The amplitude of this signal has been changed from 0.01m to 0.1m. At each value the cost function (as described in equation 23) has been calculated:

$$\phi = 0.5 \sum_{\epsilon=1}^4 z_{\epsilon}^2 \tag{23}$$

Fig. 15 shows the time response of the cost function as function of amplitude of square signal input.

B. Sine wave input signal with varying amplitude applied as road input profile

The different amplitude of sine wave input from 0.01m to 0.1m has been applied as road profile input. The time response of the cost function for the full vehicle without control, the result of optimal FOPID controller and NF controller are shown together in Fig.16.

C. Bending inertia Torque (Tx) applied

The value of bending torque (from 1000 Nm to 9000Nm) in addition to random signal as road profile has been applied. The cost function response is plotted as function of Tx in Fig. 17.

D. Breaking inertia Torque (Ty) applied

The value of breaking torque (from 1000 Nm to 9000Nm) in addition to random signal as road profile has been applied. The cost function response is plotted as function of Ty in Fig. 18.

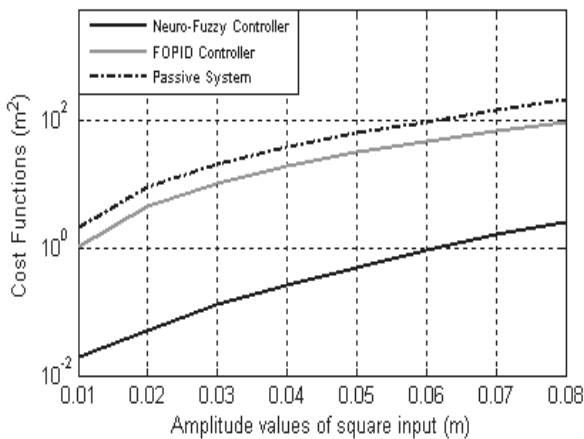


Figure 15 Time response of the cost functions against the different amplitude of square input.

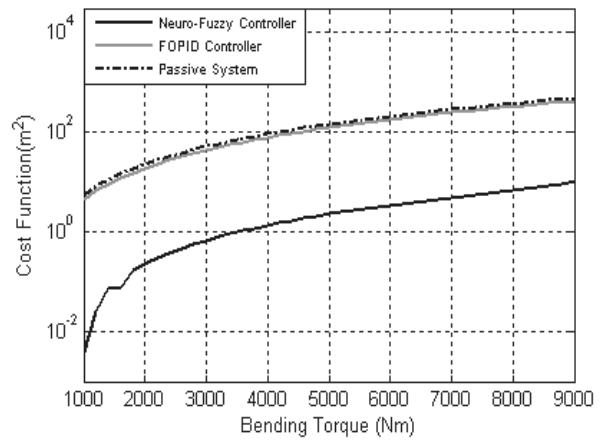


Figure 17 Time response of the cost functions against bending torque (Tx)

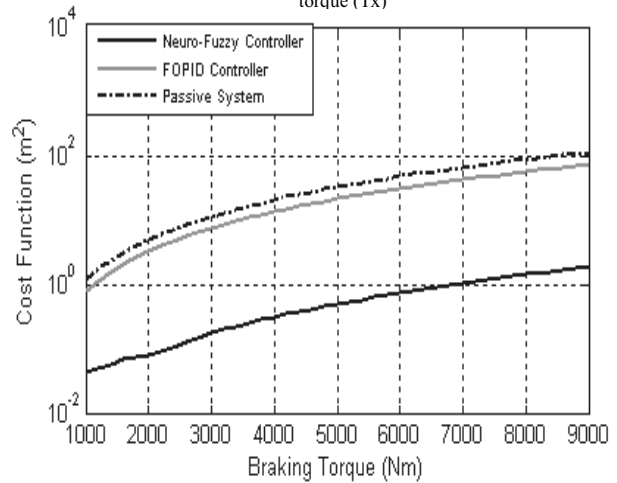


Figure 18 Time response of the cost functions against breaking torque (Ty)

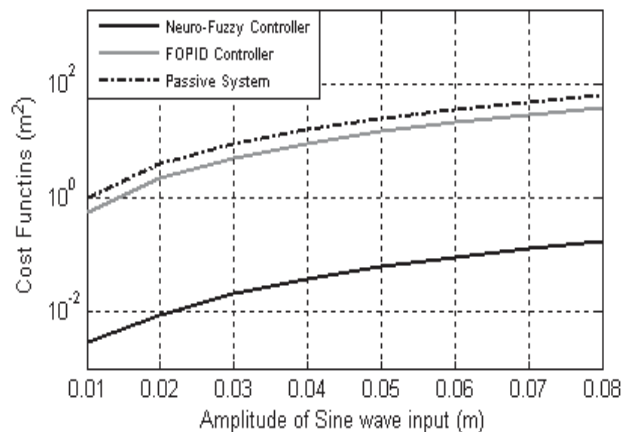


Figure 16 Time response of the cost functions against the different amplitude of sine wave input.

VII. CONCLUSION

A novel Neurofuzzy controller has been successfully developed for a full vehicle nonlinear active suspension system. The results have been compared with optimal FOPID controller and the corresponding system without controller. From these results, the NF controller has capability of minimizing the control objectives better than the optimal FOPID controller. The test of the robustness proves that the NF controller is still stable and it forces the cost function to be minimum even significant disturbances occurred. The results have been confirmed that when the NF controller has been used, the cost function is still away from zero while when the optimal FOPID controller is used the cost function has much bigger values.

REFERENCES

- [1] K. Sung, Y. Han, K. Lim and S. Choi. Discrete-time Fuzzy Sliding Mode Control for a Vehicle Suspension System Featuring an Electrorheological fluid damper. *Smart Materials and Structures* 16: pp. 798-808, 2007.
- [2] Y. Kuo and T. Li. GA Based Fuzzy PI/PD Controller for Automotive Active Suspension System. *IEEE Transactions on Industrial Electronics*, Vol. 46, No. 6: pp.1051-1056, 1999.
- [3] J. Feng and F. Yu. GA-Based PID and Fuzzy Logic Controller for Active Vehicle Suspension System. *International Journal of Automotive Technology*, Vol. 4, No. 4: pp. 181-191, 2003.
- [4] M. Smith and G. Walker. Performance Limitations and Constraints for Active and Passive Suspensions: a Mechanical Multi-port Approach, *Vehicle System Dynamics*, Vol. 33, No. 3: pp.137-168, 2000.
- [5] M. Biglarbegian, W. Melek and F. Golnaraghi. A Novel Neuro-fuzzy Controller to Enhance the Performance of Vehicle Semi-active Suspension Systems, *Vehicle System Dynamics*, Vol. 46, No.8: pp. 691-711, 2008.
- [6] M. Biglarbegian, W. Melek and F. Golnaraghi. Design of a Novel Fuzzy Controller to Enhance Stability of Vehicles, *North American Fuzzy Information Processing Society*: pp. 410-414, 2007.
- [7] L. Yue, C. Tang and H. Li. Research on Vehicle Suspension System Based on Fuzzy Logic Control, *International Conference on Automation and Logistics*, Qingdao, China, 2008.
- [8] M. Kumar. Genetic Algorithm-Based Proportional Derivative Controller for the Development of Active Suspension System, *Information Technology and Control*, Vol. 36, No. 1: pp.58-67, 2007.
- [9] Y. He and J. Mcphee. A design methodology for mechatronics vehicles: application of Multidisciplinary optimization, multimode dynamics and genetic algorithms, *Vehicle System Dynamics*, Vol. 43, No. 10: pp.697-733, 2005.
- [10] P. Gaspar, I. Szaszi and J. Bokor. Design of Robust controller for Active vehicle Suspension Using the Mixed μ Synthesis, *vehicle Dynamic System*, Vol. 40, no. 4: pp. 193–228, 2003.
- [11] A. Chamseddine, H. Noura and T. Raharjana. Control of linear Full Vehicle Active Suspension System Using Sliding Mode Techniques, *International Conference on Control Applications*, Munich, Germany, 2006.
- [12] C. March and T. Shim. Integrated Control of Suspension and front Steering to enhance Vehicle Handling, *Processing IMechE*, Vol. 221 Part D: pp. 377-391, 2006.
- [13] S. Lee, G. Kim and T. Lim. Fuzzy logic Based Fast Gain Scheduling Control for Nonlinear Suspension System, *IEEE Transaction on Industrial Electronics*, Vol. 45, No.6, pp. 953-955, 1998.
- [14] S. Li, S. Yang and W. Guo. Investigation on Chaotic Motion in Hysteretic Non-linear Suspension System with Multi-frequency Excitations, *Mechanics Research Communication* 31, pp. 229-236, 2004.
- [15] J. Dixon. "The Shock Absorber Handbook," *Society of Automotive Engineers, Inc., USA*, p. chap, 1999.
- [16] D. Joo, N. Al-Holou, J. Weaver, T. Lahdhir and F. Al-Abbas. Nonlinear Modelling of vehicle suspension System," *Proceeding of the American Control Conference*, Chicago, Illinois, 2000.
- [17] C. Isik and M. Farrokhi. Recurrent neurofuzzy system, *Annual meeting of the North American Fuzzy Information Processing Society Nafips*, 1997.
- [18] M. Brown and C. Harris. *Neurofuzzy adaptive modeling and control*, prentice hall international (UK) limited, 1994.
- [19] Y. Zhang and A. Kandel. Compensatory neurofuzzy systems with fast learning algorithms, *IEEE transactions on neural network*, Vol. 9, No. 1: pp.80-105, 1998.
- [20] H. Nguyen, N.Rasad, C.Aiker and E. Walker. *A First Course in Fuzzy and Neural Control*, USA, Chapman & Hall/ CRC, 2003.
- [21] J. Jang. ANFIS: Adaptive Network Based Fuzzy Inference System, *IEEE Transaction on System, Man and Cybernetics* 23, 665-686, 1993.
- [22] D. Xue, Y. Chen and D. Atherton. *Linear Feedback Controller Analysis and Design with MATLAB*, USA, The Society for Industrial and Applied Mathematics, 2007.
- [23] Y. Ando and M. Suzuki. Control of Active Suspension Systems Using the Singular Perturbation method, *Control Engineering Practice*, Vol. 4, No. 33, pp. 287-293, 1996.
- [24] H. Merritt. *Hydraulic Control Systems*, John Wiley and Sons, Inc, USA, 1969.
- [25] R. Rajamany and J. Hedrick. Adaptive Observers for Active Automotive Suspensions: Theory and Experiment, *IEEE Transaction on Control Systems Technology*, Vol. 3, NO. 1: pp 86-92, 1995.